Journal of Innovative Optical Health Sciences
Vol. 3, No. 1 (2010) 17–23

SDOCT IMAGE RECONSTRUCTION BY INTERFEROMETRIC SYNTHETIC APERTURE MICROSCOPY

XIAODONG CHEN*, QIAO LI, YONG LEI, YI WANG
and DAOYIN YU

*College of Precision Instrument & Opto-electronic Engineering
Tianjin University, Opto-electronic Information Science
and Technical Lab. MOE, Tianjin, 300072, China
xdchen@tju.edu.cn

Spectral domain optical coherence tomography (SDOCT) is a noninvasive, cross-sectional imaging technique that measures depth resolved reflectance of tissue by Fourier transforming the spectral interferogram with the scanning of the reference avoided. Interferometric synthetic aperture microscopy (ISAM) is an optical microscopy computed-imaging technique for measuring the optical properties of biological tissues, which can overcome the compromise between depth of focus and transverse resolution. This paper describes the principle of SDOCT and ISAM, which multiplexes raw acquisitions to provide quantitatively meaningful data with reliable spatially invariant resolution at all depths. A mathematical model for a coherent microscope with a planar scanning geometry and spectral detection was described. The two-dimensional fast Fourier transform (FFT) of spectral data in the transverse directions was calculated. Then the nonuniform ISAM resampling and filtering was implemented to yield the scattering potential within the scalar model. Inverse FFT was used to obtain the ISAM reconstruction. One scatterer, multiple scatterers, and noisy simulations were implemented by use of ISAM to catch spatially invariant resolution. ISAM images were compared to those obtained using standard optical coherence tomography (OCT) methods. The high quality of the results validates the rationality of the founded model and that diffraction limited resolution can be achieved outside the focal plane.

Keywords: Optical coherence tomography (OCT); spectral domain OCT (SDOCT); interferometric synthetic aperture microscopy (ISAM); resolution; image reconstruction.

1. Introduction

Optical coherence tomography (OCT) is analogous to ultrasonic imaging that measures the intensity of reflected infrared light rather than reflected sound waves from the sample.[1] Time gating is employed so that the time for the light to be back-reflected, or echo delay time, is used to assess the intensity of back-reflection as a function of depth. Unlike ultrasound, OCT uses an optical interferometer to measure ultra-short time delay of light back-reflected from different depths of sample.

OCT performs cross-sectional imaging by measuring the time delay and magnitude of optical echoes at different transverse positions, essentially by the use of a low coherence interferometry.[2,3] A cross-sectional image is acquired by performing successive rapid axial measurements while transversely scanning the incident sample beam onto the sample. OCT has the advantage that it can achieve extremely high axial image resolution independently of the transverse image resolution. The axial resolution is determined by the coherence length of light source which is independent of the sampling beam focusing conditions.

In the traditional reconstruction of OCT a high depth of field can be achieved at the expense of poorer transverse resolution.[4] High numerical aperture tight focusing provides better transverse resolution, but the depth of field is small. Thus trade-off between depth of focus and transverse resolution limits OCT imaging. Interferometric synthetic aperture microscopy (ISAM) is an optical microscopy computed-imaging technique for measuring the optical properties of structures and biological tissues.[4,5] ISAM makes it possible to overcome the problem by computationally inferring the susceptibility outside the focused range. The transverse image resolutions at the different depths become the same after ISAM reconstruction of OCT image. The image quality cannot degrade away from the focal plane.

In the paper, the imaging theory of spectral domain optical coherence tomography (SDOCT) is described and ISAM, which increases the transverse resolution with depth of field fixed, is analyzed. Then the reconstruction algorithm is described in a computational procedure. Next, simulations for one scatterer, multiple scatterers with gaussian white noise are carried out. ISAM images are compared to those obtained using standard OCT methods. Simulations confirm that the ISAM can makes it possible to overcome the trade-off between depth of focus and transverse resolution.

2. SDOCT Imaging Principle

The basis principle of OCT is low coherence interference.[2] In spectral domain, the full complex envelope of the depth signal of the sample is recorded to obtain spectroscopic information. The present technique uses frequency domain OCT (FDOCT), where depth resolution is obtained from backscattering spectral interferometry. FDOCT is a natural technique to directly access spectral data since by virtue of a diffraction grating the signal is already recorded in its frequency rather than space domain. Within the accuracy of the first Born approximation the three-dimensional distribution of the scattering potential of the object can be computationally reconstructed from the distribution of amplitude and phase of the light scattered by the object. The Fourier diffraction theorem relates the Fourier transform of the measured scattering data with the object structure.

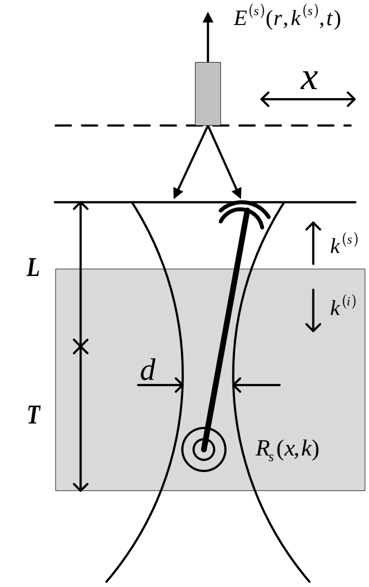

Fig. 1. The object is illuminated along the negative z-axis. $k^{(i)}$ = wavevector of illuminating light, $k^{(s)}$ = wave vector of scattered light.

2.1. *Scattering approximation*

We illuminate an object by a monochromatic (wavenumber k) Gaussian laser beam, see Fig. 1. Let the object be positioned at the beam waist and the object depth T be of the order of magnitude of the corresponding Rayleigh length. Then we can assume the object being illuminated by an approximately plane monochromatic wavefront

$$E^{(i)}(r,k^{(i)},t) = A\exp(ik^{(i)}\cdot r - i\omega t), \qquad (1)$$

where $k^{(i)}$ is the wavevector of the illuminating wave and $|k^{(i)}| = k = 2\pi/\lambda$ is the wave-number. Here we use a simplified classical description of the light beam. We ignore any field quantization and treat the electric field $\boldsymbol{E}$ of the light as a scalar, i.e. we also ignore polarization effects. Let $E^{(s)}(r,k^{(s)},t)$ be the scattered wave. The sum of the two waves $E^{(i)}(r,k^{(i)},t)+E^{(s)}(r,k^{(s)},t)$ satisfies the Helmholtz equation. In case of weakly scattering objects the scattered field can be obtained by the first Born approximation as a volume integral extended over the illuminated object volume $\boldsymbol{V}$ (r'):

$$E^{(s)}(r,k^{(s)},t) = -\frac{1}{4\pi}\int\limits_{V(r')} F(r',k^{(i)})E^{i}(r',k^{(k)},t) \times G(|r-r'|)\mathrm{d}^3r'. \qquad (2)$$

With the Green's function,

$$G(|r-r'|) = \frac{\exp(ik^{(s)}|r-r'|)}{|r-r'|}. \qquad (3)$$

We shall confine some treatment to backscattering and neglect any dispersion of the refractive index of the object, i.e. we assume the scattering potential to be independent of the wavenumber. This approximation simplifies the subsequent treatment. And we replace the three-dimensional Fourier transform of Eq. (2) by a one-dimensional Fourier transform. The scattered light has an amplitude which is proportional to the (one-dimensional) Fourier transform of the scattering potential $F(z)$ of the object potential.

$$E^{(s)}(r, k^{(s)}, t) = -\frac{A^{(i)}W}{4\pi D}\exp(ik^{(s)} \cdot r - i\varpi t) \times FT\{F(z)\}. \tag{4}$$

At P the back-scattered light wave is:

$$\begin{aligned} E^{(s)}(P, k, t) &= A^{(s)}(P, k)\exp[i\phi^{(s)}(P, k)] \\ &= -\frac{A^{(i)}W}{4\pi D}\exp(ikD - i\omega t)FT\{F(z)\}, \end{aligned} \tag{5}$$

i.e. proportional to the Fourier transform of the scattering potential. $F(z)$ can be obtained by an inverse Fourier transform of $E^{(s)}(P, k)$. Obviously this is only possible if the amplitude and phase of the scattered field $E^{(s)}(P, k)$ are known for at least a limited range of k-values. Though we only have access to the intensity of the scattered light it is clear that we have to use multi-wavelength illumination.

2.2. *Measurement of scattered field data*

As shown above the scattered light wave has to be measured for a range of wavenumbers $\boldsymbol{k}$. The wavenumber dependent intensity spectrum $I(P, k)$ of the back-scattered light is according to Eq. (5) besides a constant C — equal to the square of the Fourier transform of the scattering potential of the object:

$$I(P, k) = |E^{(s)}(P, k)|^2 = C|\mathrm{FT}\{F(z)\}|^2. \tag{6}$$

Taking the inverse Fourier transform of $I(P, k)$ yields the auto-correlation function (ACF) of the scattering potential

$$\mathrm{FT}^{-1}\{I(P, k)\} = C\langle F^*(z)F(z+Z)\rangle = C\mathrm{ACF_F}(Z). \tag{7}$$

Hence we obtain the ACF of the object scattering potential and not the object scattering potential F itself. Only with very simple object structures the ACF can be deciphered and the true scattering potential of the object can be obtained. The scattering potential can be described as a sum of the actual object $F(z)$ plus a delta-like potential (with amplitude reflectivity R):

$$F(z) = F_0(z) + R\delta(z - z_I). \tag{8}$$

Then the auto-correlation yields four terms:

$$\begin{aligned} &\langle F_0^*(z)F_0(z+Z)\rangle + \langle F_0^*(z)R\delta(z+Z-z_I)\rangle \\ &\quad + \langle R\delta^*(z-z_I)F_0(z+Z)\rangle \\ &\quad + \langle R^2\delta^*(z-z_I)\delta(z-z_I+Z)\rangle \\ &= \mathrm{ACF_F}(Z) + RF_0^*(z_I - Z) \\ &\quad + RF_0(z+Z) + R^2\delta(Z). \end{aligned} \tag{9}$$

Here the third term yields — besides the constant factor R — a true reconstruction of the object structure, centered at $z = -z_I$. A dominating light remitting interface can be realized by a reference mirror in front of the object. Any overlap between the four terms of the ACF is avoided by choosing the distance L between the interface and the object larger than the object depth $T : L > T$. So OCT depth resolved information is encoded in the cross spectral density function measured with a spectrometer located in the detection arm of an interferometer. But it must be kept in mind, that extending the depth of the object structure from T to $T + L$ increases the frequency of the Fourier transform and demands for an increased resolution in the k-space.

3. Interferometric Synthetic Aperture Microscopy (ISAM)

ISAM is an optical microscopy computed imaging technique for measuring the optical properties of three-dimensional structures and biological tissues. In the SDOCT system, the sample light is focused to some point of the sample. The lens with high numerical aperture can be used to achieve a high transverse resolution at the expense of degraded depth of field.[6] The maximum depth of imaging is invariant but images outside the focused region become blur. ISAM can make transverse resolution invariant at different planes by re-computing spectrum data; thus it eliminates the compromise between resolution and depth of field.

The SDOCT system is based on a Michelson interferometer, see Fig. 2. The light beam from a super luminance diode (SLD) is divided into two parts by a coupler. One part is the sample light. The other part is the reference light

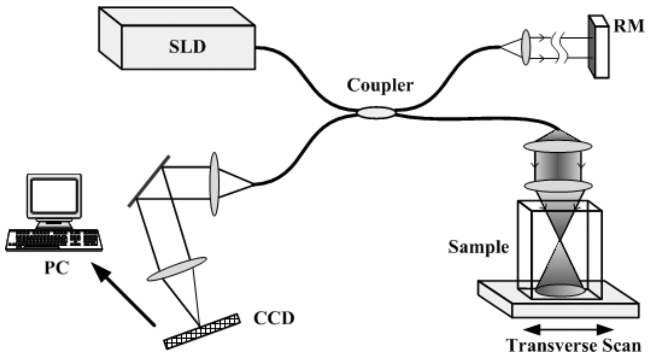

Fig. 2. Schematic of the SDOCT system. RM is reference mirror.

which is reflected by the reference mirror (RM). The back-scattered light from the sample is interfered with the reflected light from the reference arm, to be detected by a line-scan charge coupled device (CCD) array with 3648 pixels at the output of the Michelson interferometer. The spectral range is from 728.69 to 911.16 nm. The resolution of the spectroscopic detection is $\delta\lambda = 0.05\,\mathrm{nm}$, which can determine the maximum imaging depth of 3.4 mm in air. Back-scattering wave by every spots in the sample must be caught when transverse scanning. The propagation equation of the decaying wave is

$$\nabla^2 U(r) + k^2 U(r) = -4\pi\eta(r)U(r), \qquad (10)$$

where $U(\mathbf{r})$ is light field, k is wave number, and η is the scattering potential. According to the first Born approximation, the spectrum of back-scattered light is a function of the transverse position of the beam $\mathbf{r_0}$ and the wavenumber k. The expression is[4]

$$S(\mathbf{r_0}, k) = A^2(k)\int d^2r \int_V d^3r' G(\mathbf{r}', \mathbf{r}, k) \times g(\mathbf{r}' - \mathbf{r_0}, k)\eta(\mathbf{r}')g(\mathbf{r} - \mathbf{r_0}, k), \qquad (11)$$

where g is Gauss beam, $g(r,k) = W^{-2}(k) e^{-r^2/2W^2(k)}/2\pi$, $W(k) = \alpha/k, \alpha = \pi/NA$. $A^2(k)$ is the power spectral density of the source. G is the Green function, $G(r', r, k) = e^{ik|r-r'|}/|r - r'|$. After two-dimensional Fourier transform with respect to $\mathbf{r_0}$ and approximation, the signal is given by the expression

$$\tilde{S}(Q_{||}, k) = A(k)\left(\frac{i2\pi^2}{k_z(Q_{||}/2)}\frac{k^2}{\alpha^2}e^{-\frac{\alpha^2 Q^2}{4k^2}}\right) \times \tilde{\tilde{\eta}}(Q_{||}; -2k_z(Q_{||}/2)), \qquad (12)$$

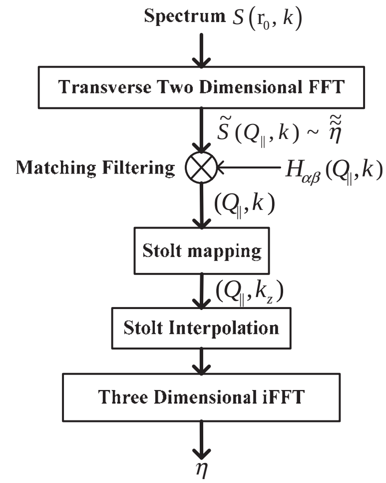

Fig. 3. The procedure of ISAM.

where $Q_{||}$ is the transverse wave vector, $k_z = \sqrt{k^2 - q^2}$, q is a variable of integration, $\tilde{\tilde{\eta}}$ is the three-dimensional Fourier transform of the scattering potential η. Because two-dimensional Fourier transform of the interference spectrum has linear relation with $\tilde{\tilde{\eta}}$, transverse resolution is independent on depth position. It will be invariant on the different depth of the sample. Because of the simple relationship, ISAM can be implemented efficiently by resampling the spectrum data as used in SAR.

According to the relationship mentioned above, the procedure of ISAM can be summarized as Fig. 3. Two-dimensional fast Fourier transform (FFT) of $S(\mathbf{r_0}, k)$ along x and y is calculated to yield $\tilde{S}(Q_{||}, k)$ in Eq. (11). Implement a linear filtering $H_{\alpha\beta}(Q_{||}, k)$ to compensate for the bandpass shape. It can be ignored when having less influence on imaging quality. Because of $Q_{||}$ has no orthogonal relation with k, Stolt mapping of $\tilde{S}(Q_{||}, k)$ is executed to yield $\tilde{S}(Q_{||}, k_z)$ in order to meet orthogonality. The mapping is $k_z = \sqrt{k^2 - q^2}$. Next, after the Stolt mapping k_z is nonuniform; it needs Stolt interpolation for the result back to a regular grid to meet FFT using cubic B splines. Then, take the inverse three-dimensional FFT and compensate for decay of the signal away from focus to get the scattering potential η(r).

4. Simulations

ISAM images are compared to results obtained using standard OCT reconstruction methods. Results show that one scatterer, multiple scatterers, and noisy reconstruction. In simulations it is supposed that the sample is composed of one or many scatterers omitting multiple scattering effect and interference among adjacent scatterers. They are placed inside and outside of the scanning boundary to simulate finite boundary conditions. The wavelength is $\lambda_0 = 1310\,\mathrm{nm}$, 3 dB bandwidth is $\Delta\lambda = 80\,\mathrm{nm}$, sampling period is $\Delta k = 0.8\,\mu m^{-1}$ from 4.4 to $5.2\,\mu m^{-1}$. There are 400 pixels in the longitudinal direction and 360 pixels in the transverse direction. Because the light intensity will decay with the penetrate depth, the scatter coefficient $R_s(z)$ has inverse relationship with the depth z in the simulations. It is given by

$$R_s(z) = \mu_b \pi (NA)^2 l_c e^{-2\mu_s z}, \tag{13}$$

where l_c is the coherence length, μ_b and μ_s are the coefficients determined by scatterer, the representative value is $\mu_b = 1.5\,\mathrm{mm}^{-1}$, $\mu_s = 5\,\mathrm{mm}^{-1}$. Furthermore, the compensation for decay of the signal away from focus is needed for the scattering potential $\eta(r)$.

4.1. *One scatterer simulations*

Figure 4 displays reconstructions with NA = 0.5, axial depth of 100, 150, and 200 μm. ISAM can also be applied for the lens with higher NA.

Results of standard OCT will become inferior as the z position of the scatterer increases. Result of ISAM is one spot at the different z position. The transverse resolution is invariant.

4.2. *Multiple scatterers simulations*

Figure 5 displays reconstructions of 100 random scatterers with NA of 0.2, 0.4, and 0.6.

For the standard OCT reconstructions it can be seen that an increase in NA provides an increase in resolution. NA has influence on results of standard OCT whose focal region becomes narrower while images of ISAM have the same transverse resolution. The spots outside the focused range are still distinct. Spots trail appears in the ISAM results (b), (d), and (f). The reason is that simulated spots

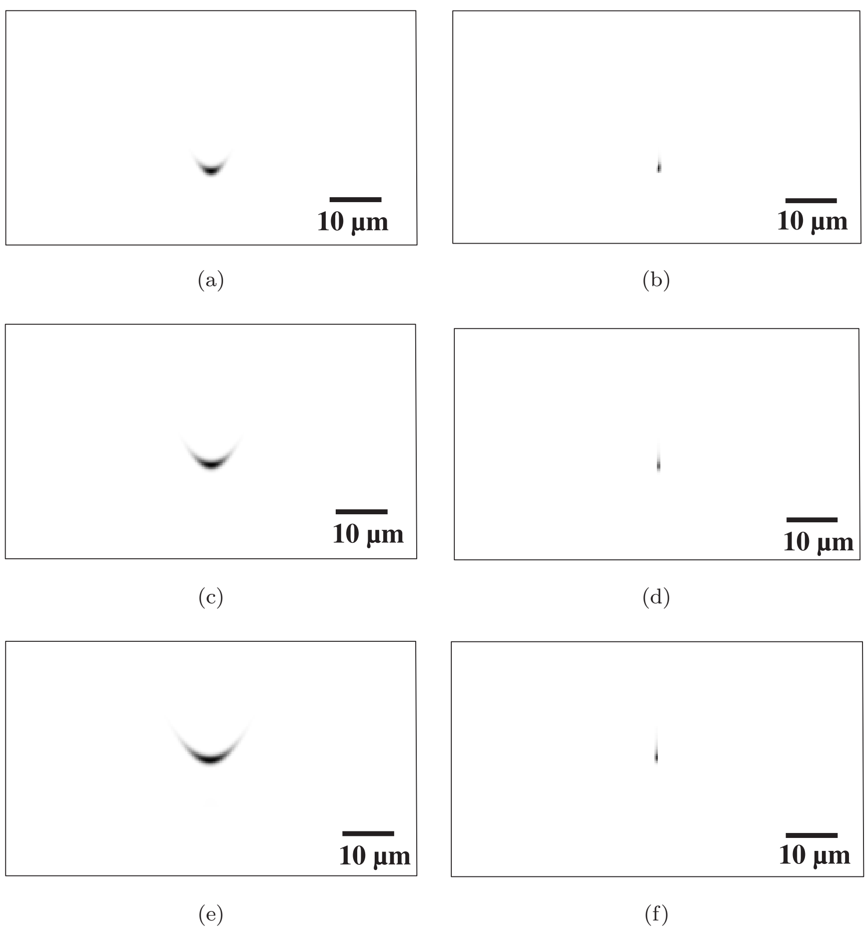

Fig. 4. Reconstructed images for one scatterer on z = 100, 150, and 200 μm. Images (a), (c), and (e) show standard OCT reconstructions. Images (b), (d), and (f) show ISAM reconstructions.

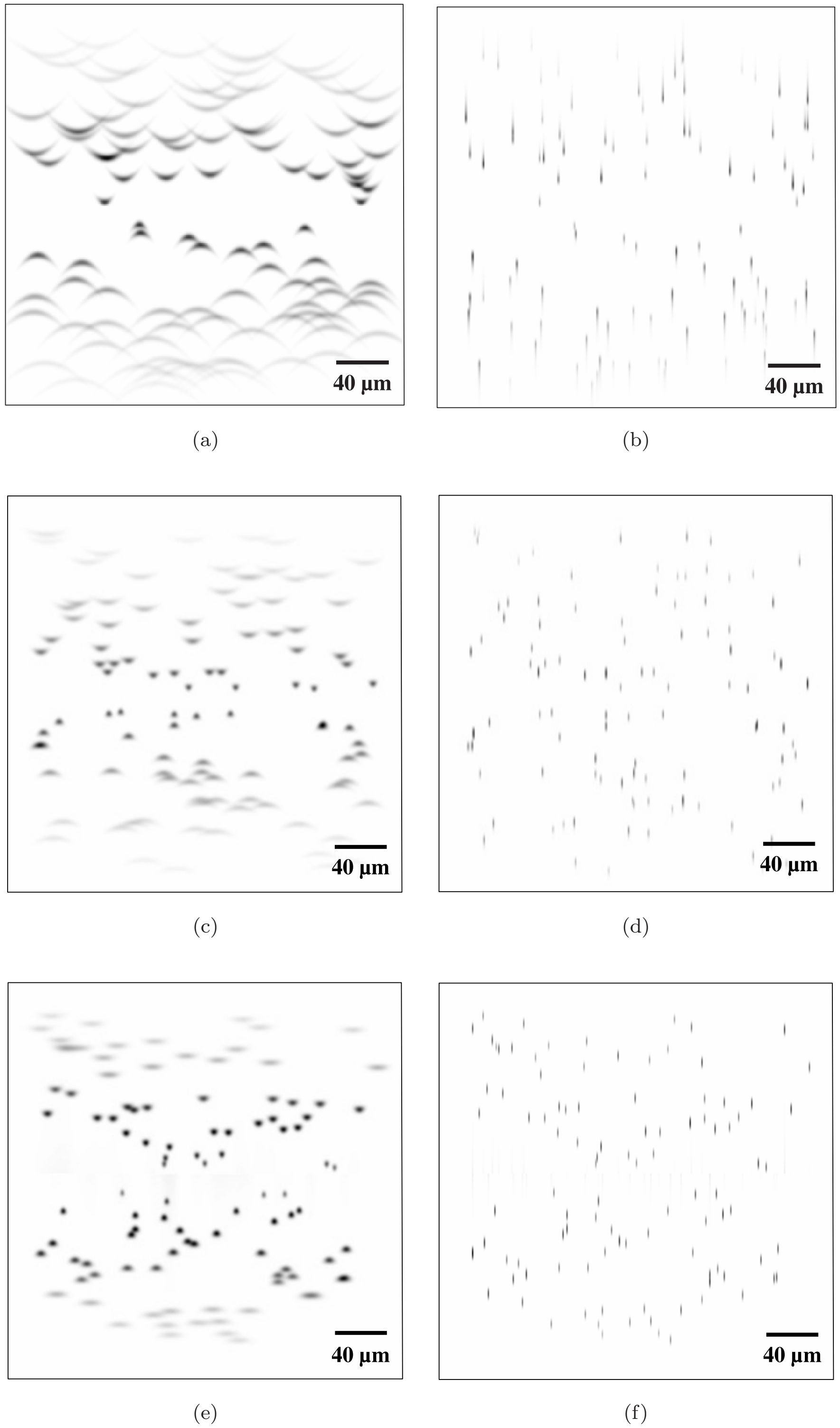

Fig. 5. Reconstruction images of 100 scatterers on NA = 0.2, 0.4, and 0.6. Images (a), (c), and (e) show standard OCT reconstructions. Images (b), (d), and (f) show ISAM reconstructions.

which are parabolic curve will have trail in the axial direction after the reconstruction. The trail will be obscure when the NA of lens is higher. It costs about 10 min to finish the 100 spots simulation using the cubic B-spline (CPU E7300 2.60GHz, 2GB RAM).

4.3. *Multiple scatterers and noisy simulations*

It is supposed that Gaussian white noise is independent of spectrum signal because the noise in

SDOCT system mainly comes from Johnson noise. The signal out of focus needs a gain which maintains the signal in the focus and out of focus planes up to a level to match the signal in the focus. However, the gain also amplifies noise; thus focal region is dependent of noise not NA. In the high noisy system, the intensity on the focal plane is corresponded with the noisy intensity. Now the signal far from the focal plane will vanish even after ISAM reconstruction. It has the same focal depth as the standard OCT. In a low noisy system, ISAM has much effect on expanding focal region. All the scatterers in the sample are visible until they are out of focal region and are submerged by noise. In Fig. 6 an object consisting of 100 spots scatterers is considered. For a well-designed OCT/ISAM system and an appropriate sample, it is reasonable to expect a relatively high SNR, as SDOCT systems have reported sensitivities of greater than 80 dB.[5] Therefore the noise level considered results in SNR values of 40 dB.

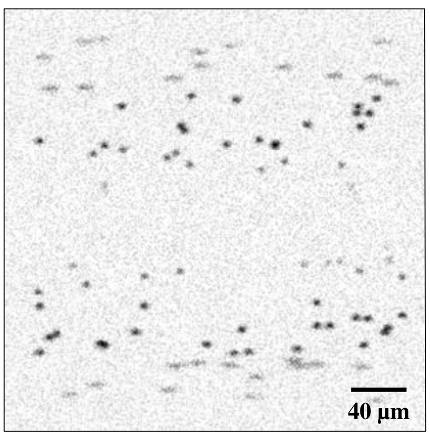

(a)

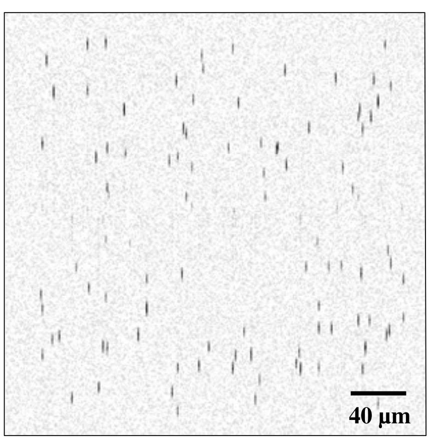

(b)

Fig. 6. Noisy reconstruction images of 100 scatterers. OCT reconstructions are shown on the left and ISAM reconstructions on the right. The noise level considered results in SNR values of 40 dB and NA = 0.6.

5. Conclusions

OCT is a noninvasive, cross-sectional imaging technique that measures depth resolved reflectance of tissue. In SDOCT low-numerical aperture optics are used to achieve a high depth of field at the expense of degraded transverse resolution. ISAM is a computed imaging technique that quantitatively estimates a three-dimensional scattering object in broadband coherent microscopy. The nonuniform ISAM resampling and filtering is implemented to yield the scattering potential within the scalar model. Inverse FFT is used to obtain the ISAM reconstruction. ISAM images are compared to those obtained using standard OCT methods. Increasing the NA of the objective lens does not reduce the depth of focus; it increases only resolution and signal level in the in-focus region.

References

1. D. Huang, E. A. Swanson, C. P. Lin, "Optical coherence tomography," *Science* **254**(5035), 1178–1181 (1991).
2. J. G. Fujimoto, "Optical coherence tomography: Technology and applications," *IEEE Optical MEMs*, **1031485**, 147–148 (2002).
3. J. G. Fujimoto, "Optical coherence tomography," *Appl. Phys.*, **2**, 1099–1111 (2001).
4. T. S. Ralston, D. L. Marks, P. S. Carney, S. A. Boppart, "Interferometric synthetic aperture microscopy," *Nat. Phys.* **5**, 129–134 (2007).
5. B. J. Davis, S. C. Schlachter, D. L. Marks, T. S. Ralston, S. A. Boppart, P. S. Carney, "Nonparaxial vector-field modeling of optical coherence tomography and interferometric synthetic aperture microscopy," *J. Opt. Soc. Am. A* **24**(9), 2527–2542 (2007).
6. T. S. Ralston, D. L. Marks, S. A. Boppart, P. S. Carney, "Inverse scattering for high-resolution interferometric microscopy," *Opt. Lett.* **31**, 3585–3587 (2006).